Scholar Publishing Group
Frontiers in Ocean Engineering
https://doi.org/10.38007/FOE.2020.010301
ISSN 2790-2706 Vol. 1, Issue 3: 1-9

Marine Engineering Water Environment based on Numerical Simulation Analysis

Mathea Simons*

Univ Batna2, Comp Sci Dept, LaSTIC Lab, Batna 05078, Algeria

**corresponding author*

Keywords: Numerical Simulation Analysis, Ocean Engineering, Water Environment, Application Research

Abstract: With the rapid development of economy and society, the large-scale reclamation projects not only provide valuable land resources for human beings, but also easily have a great impact on the local WE conditions, which may lead to the continuous destruction of coastal wetlands and natural coastlines, the decline of self purification capacity of seawater, the weakening or even blocking of material and energy exchange with the open sea, and ultimately the destruction of the local ecological environment, This has seriously restricted the sustainable development of the local economy and society. The marine engineering water environment(MEWE) has become the current research hotspot. Therefore, this paper studies and analyzes the application of numerical simulation(NS) in the MEWE. The establishment of ocean water quality model, water quality characteristics and hydrodynamic characteristics of ocean engineering are analyzed. Taking Laizhou Bay as the research object, numerical simulation analysis(NSA) is applied to the WE of ocean engineering, and experimental test analysis is carried out. The experimental results show that the application of NSA to the MEWE has important guiding significance for improving the MEWE monitoring.

1. Introduction

With the rapid development of modern industry and agriculture, industrial wastewater, pesticides, chemical fertilizers and industrial and agricultural wastes have become the important reasons that damage the drinking WE. The impact of human lifestyles on the marine environment is becoming more and more serious, which directly leads to the destruction of the marine environment and the living environment, and seriously interferes with the normal survival of marine animals, and also restricts the rapid development of China's aquaculture industry. However, in recent years, the phenomenon of marine environment has gradually received the attention of the whole world. Countries around the world have issued active policies to protect the marine environment. The analysis of MEWE has become an urgent and arduous task. This paper applies NSA to the MEWE

and conducts Research on it.

In the field of numerical model research, foreign countries started earlier and have rich work results. Among them, the offshore waters are the most concerned by the majority of scholars. It generally refers to the areas most closely related to human production and life, such as the continental shelf, estuaries and coastal bays. Many scholars have studied and analyzed the application of NSA in MEWE. On the basis of analyzing the existing data and combining the characteristics of regional karst groundwater recharge, runoff and discharge, Zhang established a NS model of sanguquan basin by using visual software. The karst groundwater resources and groundWE in the basin under different mining schemes are evaluated, and the changes of karst groundWE in the next 10 years are predicted [1]. Simionov I a has ideal fitting effect for the sanguquan basin with complex lithology and structure. The flow field and salinity field in the Gulf of the United States are successfully simulated by using the three-dimensional tidal current control equation expressed in tensor form. At this stage, the research on numerical models of Estuary and coast in China has also developed rapidly, and many research results have been obtained. A three-dimensional tidal current mathematical model has been constructed to successfully simulate the tidal current field of the Yangtze Estuary [2].

With the development of the mathematical model of environmental fluid mechanics and the improvement of computer computing ability, a large amount of data can be generated in the process of NS. The NSA in this paper is based on the characteristics of the MEWE. During the pretreatment, the water body or pollutants are appropriately traced, and then the calculation results are statistically analyzed to reduce the amount of data and extract useful information [3-4].

2. Analysis of MEWE

2.1. Establishment of Marine Water Quality Model

The water quality model is a quantitative description of the time and space of pollutants through computer NS. In a certain water system, it is generally difficult to obtain the data about water layer change prediction through field tests. Due to the problems of cost and environmental impact in the physical model, the water quality NS has become the most commonly used method to simulate the real natural WE system [5-6].

The current water quality model has done detailed work in many aspects. Combined with the knowledge of Microbiology, physical chemistry and other disciplines, it can calculate the migration and diffusion laws of E. coli and other substances from the external light intensity, ultraviolet intensity, temperature and wind speed, and air environment [7-8]. For the migration, diffusion and attenuation in large rivers, the pollutants discharged from the bank need to go through a long distance to achieve uniform distribution on the cross section. The WE simulation in the mixing area can be described by a two-dimensional model. For any pollutant, it can be solved by coupling a pollutant transport equation [9-10].

2.2. Analysis of Water Quality Characteristics of Offshore Engineering

The natural neighborhood interpolation method can find the input sample subset closest to the query point, and apply weight to these samples based on the area size. The interpolation method only uses the sample subset around the query point, ensuring that the interpolation height is within the range of the used samples and is smooth at all positions except the input sample position. This interpolation method can reflect the actual value range of pollutants and the spatial distribution of pollutants in each sampling interval [11-12].

Inorganic nitrogen the inorganic nitrogen in seawater is the sum of nitrate, nitrite and ammonia

concentrations. The inorganic nitrogen content of all stations in the surveyed sea area exceeds the class II sea water quality standard specified in the marine functional zoning of the area, and its spatial distribution shows a trend of decreasing from the near shore to the open sea. The pollution degree in the northern sea area is obviously stronger than that in the Southern sea area. The most serious pollution areas are the western channel outside the Wanggang estuary and the sea area outside the Xiaoyang estuary.

Active phosphates the active phosphates in the ocean mainly come from urban domestic sewage, chemical fertilizer, food, industrial wastewater, farmland drainage and aquaculture wastes. As an indicator of the content of organic pollutants in the water body, COD can indirectly reflect the degree of organic pollution in the water body. The larger the COD value, the more serious the organic pollution in the water body [13]. The maximum value occurs in the coastal waters where the main areas exceeding the standard are located. The more serious pollution is the belt shaped area formed by the outer sea area of xiaoyangkou, Dongdagang and Western waterways.

The oil pollutants in the oil ocean mainly come from the oil exploitation, transportation, loading and unloading, processing, ballast water discharge of ships and land-based sewage discharge [14-15]. Most of the surveyed sea areas are beyond the standard. The formation of the two high value areas is due to the influence of the high value of the surveyed stations. According to the data collection, there are no offshore oil exploration projects in the areas where the two stations are located. The specific reasons for the high value still need to be further studied.

2.3. Analysis of Hydrodynamic Characteristics

Analysis of fluctuation tidal current velocity and flow direction. The flow direction is affected by the rotating tidal wave and the forward tidal wave of the East China Sea. The sea water in the study area shows the form of convergence and divergence at the ebb tide. During the flood tide, the south sea water propagates to the northwest or northwest along the main tidal troughs such as the rotten sand ocean and the yellow sand ocean, and enters the tiaozi mud water area and flows up to the tidal flat; The northern sea water flows from north to south along the large tidal main troughs such as the Western Ocean, chenjiawu trough and Kushui ocean. After approaching the central part, the peripheral main troughs turn to the West and southwest, enter the tiaozi mud water area and flow up to the tidal flat. The flow path of seawater at ebb tide is the same as that at flood tide, and it is divergent outward from the strip mud [16]. Due to the limitation of tidal channels between sandbanks, the rising and falling tides in the radiated sandbanks are at the peak of Weigang, showing a relatively obvious reciprocating flow pattern.

According to the flow direction of the rising and falling tide, 14 tidal observation points are selected on the main tidal channels and sandbanks around the inner edge area of the radial sandbar. According to the established two-dimensional tidal mathematical model above, the average flow velocity during spring and autumn tide is calculated and the flow velocity difference in the area is analyzed. During the rising and falling tides, the velocity of tidal channels such as the western channel, the rotten sand ocean, the yellow sand ocean, the Kushui ocean and the chenjiawu trough is significantly higher than that on the sandbanks such as Dongsha, gaoni and tiaozi [17-18].

3. Application of NSA in MEWE

Generally, the open boundary can be calculated with a given water level, flow velocity or discharge, and the tidal level boundary is the most common. If there are measured data near the open boundary, the open boundary conditions shall be calculated according to the measured data. If there is no data for direct application, the nested model layer by layer shall be used to calculate the conditions at the target boundary from the mature large model. For the tidal level boundary, the

boundary conditions are given by the following formula according to the harmonic constants of each tidal component:

$$\lambda = H_{mean} + \sum_{i=1}^{n} a_i \cos(v_i t - \xi) \tag{1}$$

Where: n is the total tidal component, AI, VI ξ I still represents the amplitude, frequency and delay angle of the ith tidal component, and hmean is the water level of the point relative to the mean sea level.

$$\begin{aligned} \lambda(x,y,z,t)\big|\sigma_2 &= \eta^*(x,y,z,t) \\ \overline{K}(x,y,z,t)\big|\sigma_2 &= \overline{K}^*(x,y,z,t) \\ G(x,y,z,t)\big|\sigma_2 &= G^*(x,y,z,t) \end{aligned} \tag{2}$$

Where: is the open boundary, (x, y, Z, t), (x, y, Z, t), (x, y, Z, t) are the known water level, flow rate and flow rate respectively.

The so-called dynamic boundary refers to the process that the water land boundary is always in dynamic change with the action of tide. The model will monitor the water depth value of each unit in real time, judge the water depth type of each unit at each time and classify it according to the predefined dry water depth, submerged water depth and wet water depth values, and find out the position of the water boundary accordingly. When the water depth of the grid unit is less than the dry water depth and in the beach state, the model will remove the unit so that it does not participate in the calculation; When the water depth of the grid element is greater than the dry water depth and less than the wet water depth, the model sets the momentum flux of the element to 0, and only considers the mass flux to participate in the calculation.

Free surface boundary. When the surface layer, C= λ When:

$$\frac{\delta\lambda}{\delta t} + \gamma\frac{\delta\lambda}{\delta x} + w\frac{\delta\lambda}{\delta y} - v = 0, \left(\frac{\delta\gamma}{\delta c}, \frac{\delta w}{\delta c}\right) = \frac{1}{\rho_0 w_i}(\sigma_{sx}, \sigma_{sy}) \tag{3}$$

Where, the shear stress generated by the wind on the free surface in the X and Y directions = (,) can be obtained by the following empirical formula:

$$\overline{\sigma}_s = \rho_n b_d |\gamma_v| \overline{\gamma}_v \tag{4}$$

Where, is the atmospheric density and is the atmospheric drag coefficient.

4. Application of NSA to Experimental Test and Analysis of MEWE

4.1. Composition of Nutrients in MEWE

By comparing the actual n / P ratio of the target ocean with the Redfield number, this paper studies the composition of marine nutrients in Laizhou Bay. The measured data in Table 1 shows that since the 1980s, the composition proportion of nutrients has changed greatly, and the N / P ratio has been increasing. In the 21st century, with the large increase of inorganic ammonia content and the large reduction of phosphate in rivers entering the sea, the N / P ratio in the Bay has increased more rapidly. The average value of N / P ratio in Laizhou Bay is close to 150. By 2010, the average value of N / P ratio has been close to 300. From a long-term perspective, the phosphorus limit still has a trend of further aggravation.

Table 1. Composition of marine nutrients

time	Water layer	Measured N/P	Simulation N/P
May	surface	133.3	35.74
	bottom	143.3	33.67
	average	136	34.75
October	surface	51.6	49.96
	bottom	47.4	31.12
	average	49.4	40.53

4.2. NSA Test

In order to better analyze the impact of the two rivers on the water quality of Laizhou Bay, and explore the role of nutrient composition on the growth of phytoplankton, the following two groups of numerical experiments were conducted around the limitation of nutrient in Laizhou Bay: the din and pot of the two sources of the Yellow River and Xiaoqing River were expanded by 5 times respectively to analyze the effect of nutrient composition on the growth of plankton cattle; The input of nitrogen and phosphorus nutrients from the point sources of the Yellow River and the Xiaoqing River was closed (other state variables remained unchanged) to study the contribution of these two important nutrient point sources to the nutrient level and phytoplankton cattle length in Laizhou Bay.

Table 2. Numerical test a chlorophyll content statistics

month	Normal situation	5x DIN		5x PO4	
	Mean CHL (mg /)	Mean CHL (mg / L)	Change rate (%)	Mean CHL (mg / L)	Change rate (%)
January	0.001132	0.001068	-5.69	0.001584	39.97
February	0.001556	0.001539	-1.09	0.001875	20.51
March	0.001959	0.001995	1.82	0.002137	9.08
April	0.001747	0.001789	2.37	0.001 886	7.98
May	0.001267	0.001348	6.43	0.001363	7.60
June	0.000947	0.001015	7.08	0.001099	16.00
July	0.000818	0.001023	25.16	0.000882	7.91
August	0.001239	0.001513	22.17	0.001343	8.39
September	0.001138	0.001336	17.38	0.001230	8.06
October	0.001215	0.001233	1.46	0.001735	42.77
November	0.001082	0.001067	-1.41	0.001801	66.44
December	0.001314	0.001391	6.78	0.001580	21.35

Table 2 shows the data statistics of numerical test A. under normal conditions, the annual

average chlorophyll content is 1.314mg/m3. After the point source din and P04 are expanded five times, the annual average chlorophyll content is 1.91mg/m3 and 1.58mg/m3, respectively, with an increase of 6.78% and d21.35%. It can be seen that the contribution of inorganic phosphorus to the growth of floating plants is higher than that of inorganic nitrogen, that is, from the perspective of the average of the whole sea area, The limitation of inorganic phosphorus is the main problem of nutrient limitation in Laizhou Bay; The increase of inorganic nitrogen can also cause the increase of phytoplankton content, which also shows that although the overall average nutrient level in Laizhou Bay is limited by phosphorus, there are also nitrogen limitations in some sea areas.

Table 3. Table of average chlorophyll concentration change data

	1	2	3	4	5	6	7	8	9	10
Normal situation	0.0011	0.0015	0.0018	0.0017	0.0014	0.0008	0.0007	0.0012	0.0011	0.0016
Close Xiaoqing River	0.0012	0.0015	0.0019	0.0017	0.0014	0.0007	0.0006	0.0011	0.0010	0.0015
Close the Yellow River	0.0012	0.0017	0.0020	0.0017	0.0011	0.0004	0.0003	0.0006	0.0007	0.0009

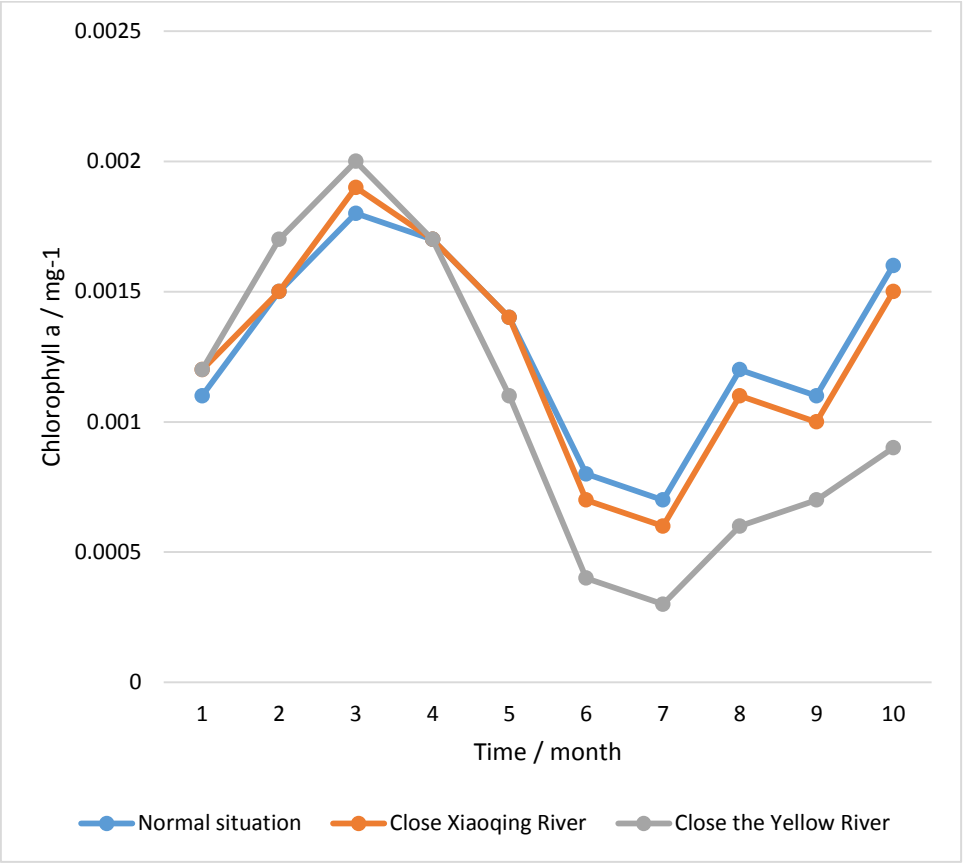

Figure 1. Variation process of monthly average chlorophyll concentration in Laizhou Bay

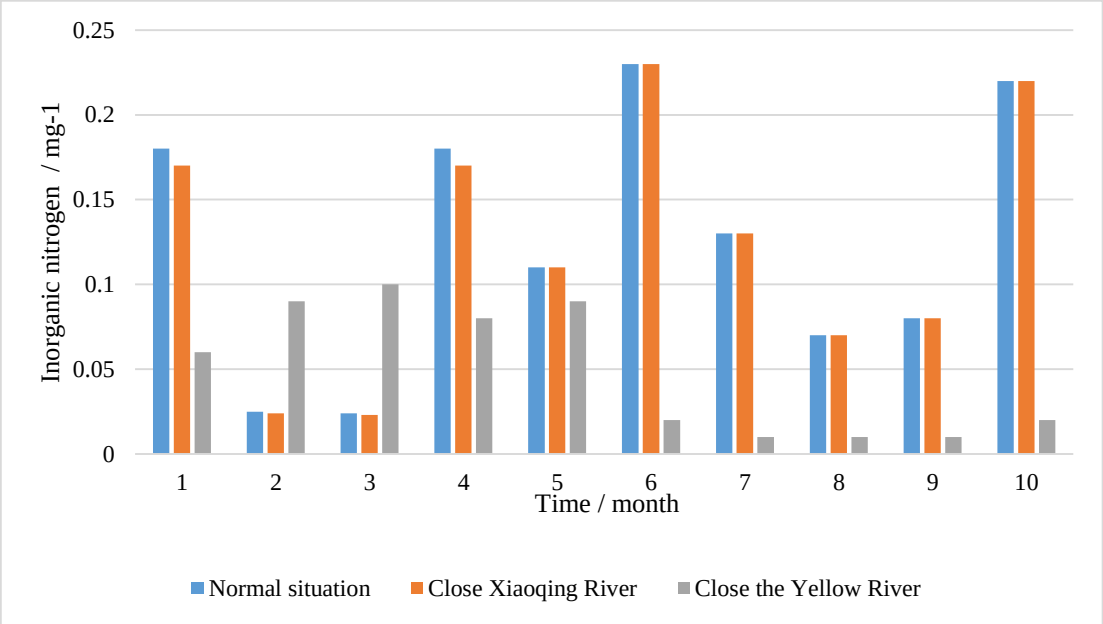

Figure 2. Variation process of monthly average nutrient concentration in Laizhou Bay

The results of numerical test B are shown in Fig. 1 and Fig. 2. The general trend of chlorophyll a content change is still consistent. The impact of Xiaoqing River point source on d1n, P04 and Chl a in Laizhou Bay is weaker than that of the Yellow River point source. When the point source of Xiaoqing River is closed, the din content in Laizhou Bay is basically unchanged, and the POA content has a slight decrease, Po. The decrease of Chl-a caused the growth of phytoplankton to be more restricted, which also caused a slight decrease of Chl-a content. The annual intake of DIN in Xiaoqing River only accounts for about 10% of that in Laizhou Bay. It is not the main source of DIN nutrients in Laizhou Bay, so it will not have a great impact on the level of inorganic salts such as nitrogen and phosphorus in Laizhou Bay. When the point source of the Yellow River is closed, the din content in Laizhou Bay decreases significantly. This is because the annual intake of DIN in the Yellow River accounts for 85% of that in Laizhou Bay. The large reduction of DIN may change the average nutrient level in Laizhou Bay from phosphorus limitation to nitrogen limitation, weakening the growth of phytoplankton restricted by inorganic nitrogen, and further reducing the absorbed P04 content. Therefore, when the point source of the Yellow River is closed, the din content decreases significantly, However, the content of P04 increased obviously. Except for a slight abnormal increase in February and March, the content of Chl-a decreased in other months, especially from June to November, so that the second peak of phytoplankton bloom in autumn almost disappeared.

5. Conclusion

This paper mainly analyzes the application of NS in MEWE. Through the detection and analysis of DIN, PO4 and other contents in marine water quality, the experimental analysis is carried out, and the accuracy of the measured results is high. However, the application of mathematical simulation in the environmental impact assessment of marine engineering water quality must be distorted to some extent. What it needs is to omit or ignore certain factors under ideal conditions, which is a summary of experience. Some hypothetical conditions have a great impact on the accuracy of NS. The mathematical model is effective for the phenomena with certain rules and regulations, and can maintain certain continuity in time and space. Due to the influence of the

environment or its own factors, the error is relatively large. NS is an important technical method for the study of coastal ocean tidal current and sediment movement. Therefore, the application of NSA in the MEWE needs further research.

Funding

This article is not supported by any foundation.

Data Availability

Data sharing is not applicable to this article as no new data were created or analysed in this study.

Conflict of Interest

The author states that this article has no conflict of interest.

References

[1] ZHANG, Chun-Chao H , Xin-Wei L , et al. Numerical simulation and environmental impact prediction of karst groundwater in Sangu Spring Basin, China. Journal of Groundwater Science and Engineering, 2020, v.8;No.30(03):20-32.

[2] Simionov I A , Cristea V , Petrea S M , et al. evaluation of heavy metals concentration dynamics in fish from the black sea coastal area: an overview. Environmental engineering and management journal, 2019, 18(5):1097-1110. https://doi.org/10.30638/eemj.2019.106

[3] Hasan S R , Karim M M . Revised energy efficiency design index parameters for inland cargo ships of Bangladesh. Proceedings of the Institution of Mechanical Engineers, Part M: Journal of Engineering for the Maritime Environment, 2020, 234(1):89-99. https://doi.org/10.1177/1475090219863956

[4] Obasi R A , Madukwe H Y , Olaosun T . Source Area Weathering, Paleo-Environment and Paleo-Climatic Conditions of Soils from Bitumen Rich Ode Irele Area of Ondo State, Nigeria. European Journal of Engineering Research and Science, 2019, 4(3):59-67. https://doi.org/10.24018/ejers.2019.4.3.1159

[5] Lee J W , Choi Y H , Kim Y B , et al. A Study on Position Estimation and Path Planning Technology of Autonomous Underwater Vehicle (AUV). Journal of Power System Engineering, 2020, 24(3):60-66. https://doi.org/10.9726/kspse.2020.24.3.060

[6] Natu A , Garg V , Badhwar A , et al. Modeling and Development of an Autonomous Underwater Vehicle ARYA for Object Recognition. International Journal of Recent Technology and Engineering, 2019, 8(2):5505-5510. https://doi.org/10.35940/ijrte.B2843.078219

[7] Ayaz M , Aggoune H M , Ammad-Uddin M . Mobile unsupervised platform for real-time ocean water quality monitoring. Control Engineering and Applied Informatics, 2019, 21(1):79-88.

[8] Heshmati-Alamdari S , Nikou A , Dimarogonas D V . Robust Trajectory Tracking Control for Underactuated Autonomous Underwater Vehicles in Uncertain Environments. IEEE Transactions on Automation Science and Engineering, 2020, PP(99):1-14. https://doi.org/10.1109/CDC40024.2019.9030165

[9] Goncalves G , Andriolo U , Pinto L , et al. Mapping marine litter using UAS on a beach-dune system: a multidisciplinary approach. The Science of the Total Environment, 2020, 706(Mar.1):135742.1-135742.14. https://doi.org/10.1016/j.scitotenv.2019.135742

[10] Liu Z , Takahashi T , Lindsay D , et al. Digital In-Line Holography for Large-Volume Analysis

of Vertical Motion of Microscale Marine Plankton and Other Particles. IEEE Journal of Oceanic Engineering, 2020, PP(99):1-13.

[11] Alizadeh F , Kharghani N , Soares C G . Effect of long-term moisture exposure on impact response of glass-reinforced vinylester:. Proceedings of the Institution of Mechanical Engineers, Part M: Journal of Engineering for the Maritime Environment, 2020, 235(4):854-865. https://doi.org/10.1177/1475090221996167

[12] Viet P V , Hoang A T . Technological Perspective for Reducing Emissions from Marine Engines. International Journal on Advanced Science Engineering and Information Technology, 2019, 9(6):1989-2000. https://doi.org/10.18517/ijaseit.9.6.10429

[13] Asuelimen G , Blanco-Davis E , Wang J , et al. Formal Safety Assessment of a Marine Seismic Survey Vessel Operation, Incorporating Risk Matrix and Fault Tree Analysis. Journal of Marine Science and Application, 2020, 19(2):155-172. https://doi.org/10.1007/s11804-020-00136-4

[14] Najafi M , Darvizeh A , Ansari R . Effect of salt water conditioning on novel fiber metal laminates for marine applications:. Proceedings of the Institution of Mechanical Engineers, Part L: Journal of Materials: Design and Applications, 2019, 233(8):1542-1554. https://doi.org/10.1177/1464420718767946

[15] Kumar T S , Reddy S , Babu K C , et al. Performance of CO 2 Cured Sugar Cane Bagasse Ash Concrete in Marine Environment. Civil Engineering and Architecture, 2020, 8(5):771-776. https://doi.org/10.13189/cea.2020.080504

[16] Umesh P A , Bhaskaran P K , Sandhya K G , et al. Numerical simulation and preliminary analysis of spectral slope and tail characteristics using nested WAM-SWAN in a shallow water application off Visakhapatnam. Ocean Engineering, 2019, 173(FEB.1):268-283. https://doi.org/10.1016/j.oceaneng.2018.12.034

[17] Koellermeier J , Rominger M . Analysis and Numerical Simulation of Hyperbolic Shallow Water Moment Equations. Communications in Computational Physics, 2020, 28(3):1038-1084. https://doi.org/10.4208/cicp.OA-2019-0065

[18] Ashraf S , Ahmad A , Yahya A , et al. Underwater routing protocols: Analysis of link selection challenges. AIMS Electronics and Electrical Engineering, 2020, 4(3):234-248. https://doi.org/10.3934/ElectrEng.2020.3.234